# Local density approximation for the relativistic nucleon-nucleus potential

M. Jaminon
*Institut de Physique B5, Université de Liège, Sart Tilman, 4000 Liège 1, Belgium*
(Received 4 June 1982)

We investigate the relativistic Hartree-Fock single-particle potential in the framework of a local density approximation and of an improved local density approximation. In most cases the latter yields a better agreement between theoretical and experimental results for quantities which are characteristic of the nuclear surface. In the case of $^{40}$Ca, the energy dependence of the ratio of the strengths of the scalar and vector components of the relativistic potential in the center-of-mass system is in good agreement with that determined by the elastic scattering data analyses. In keeping with recent experimental evidence, the calculated central part of the optical-model potential has a wine-bottle bottom shape at intermediate energy. Both approximations provide a strong spin-orbit component.

[ NUCLEAR REACTIONS Improved local density approximation for the relativistic Hartree-Fock single-particle potential in $^{40}$Ca. ]

## I. INTRODUCTION

In the last decade, many attempts have been made to derive a relativistic quantum field theory which would describe properties of finite nuclei and of nuclear matter. This renewed interest finds its origin in the work of Miller and Green,[1] who investigated ground state properties of doubly-magic spherical nuclei, and of Walecka[2] who developed a simple mean-field approach for nuclear matter. In particular, Miller and Green[1] have established that a *Hartree self-consistent* approach, including the exchange of only two neutral mesons between nucleons, namely the scalar meson $\sigma$ and the vector meson $\omega$, yields a rather good agreement between calculated and experimental values of binding energies and of the radial charge distributions. Correspondingly, we have found that the Hartree approximation also provides a good description for scattering states.[3] To go one step further in the perturbation theory, one has to include the Fock contribution in the average nucleon-nucleus potential. Miller[4] has shown that this average Hartree-Fock potential ($U^{\mathrm{HF}}$) can always be made local, but is then state dependent. For a spherical nucleus, symmetry considerations imply that it is the sum of only four Lorentz components whatever the nature of the exchanged mesons: a scalar ($U_s$), the fourth component of a vector ($U_o$), a spatial component ($U_v$), and a tensor component ($U_T$). The Hartree-Fock-Dirac equation satisfied by the single-nucleon wave function $\phi(\vec{r};\epsilon)$ is then written

$$\{\vec{\alpha}\cdot\vec{p}+\gamma^0[m+U^{\mathrm{HF}}(r)]\}\phi(\vec{r};\epsilon) = (\epsilon+m)\phi(\vec{r};\epsilon) \quad (1.1)$$

with

$$U^{\mathrm{HF}}(r)=U_s^{\mathrm{HF}}(r)+\gamma^0 U_o^{\mathrm{HF}}(r) + \gamma^r U_v^{\mathrm{HF}}(r)+\gamma^0\gamma^r U_T^{\mathrm{HF}}(r)\,. \quad (1.2)$$

For simplicity, we have not indicated the state dependence of the various components. Work[5] is in progress in order to estimate these components exactly, but the self-consistent calculation appears quite difficult. Therefore we have found it useful to develop an intermediate step which amounts to calculating the Lorentz components in the Hartree-Fock mean field approximation for symmetric nuclear matter.[6] Here, we use a local density approximation in order to obtain the values of the Hartree-Fock potentials for a finite nucleus. In our investigations, we only have included the exchange of the mesons $\sigma$ and $\omega$. Previously, Arnold and Clark[7] had used a local density approximation in order to compare predictions of a relativistic *Hartree* model with properties of the nonrelativistic optical model.

In this paper, we briefly recall the definition of the usual local density approximation[3,6,8] (Sec. II A) and we exhibit why some properties of nuclei are not well reproduced with this approximation (Sec. II B). In Sec. III we introduce an *"improved" local*

 

*density approximation* which better reproduces the surface properties of the nucleus. Section IV is devoted to numerical results. We first define the input parameters used in our calculations (Sec. IV A). In Sec. IV B, we study the energy dependence of the strengths of the scalar ($U_s$) and vector ($U_o$) components of the single-particle potential. In Sec. IV C, we investigate the radial shape of the central part of the Schrödinger-equivalent potential[9] at intermediate energy, and the energy dependence of its volume integral and of its mean square radius. We also show results for its spin-orbit component. Finally, Sec. V contains a brief summary.

## II. LOCAL DENSITY APPROXIMATION

### A. Definition

In Ref. 6, we have shown that in nuclear matter the relativistic Hartree-Fock single-particle potential (1.2) reduces to the sum of only three well-defined Lorentz components: a scalar, the fourth component of a vector, and a spatial component

$$U^{\mathrm{HF}}(k_F,\vec{k})=U_s^{\mathrm{HF}}(k_F,k)+\gamma^0 U_o^{\mathrm{HF}}(k_F,k)+\vec{\gamma}\cdot\frac{\vec{k}}{k}U_v^{\mathrm{HF}}(k_F,k) \tag{2.1}$$

with ($i=o,s$),

$$U_i^{\mathrm{HF}}(k_F,k)=U_i^H(k_F)+U_i^F(k_F,k)\ , \tag{2.2}$$

$$U_v^{\mathrm{HF}}(k_F,k)=U_v^F(k_F,k)\ . \tag{2.3}$$

In Eqs. (2.1)–(2.3) we have indicated explicitly the dependence of the fields upon the Fermi momentum $k_F$ and upon the momentum $k$ of the incident nucleon. The upper indices $H$ and $F$ refer to the Hartree and Fock contributions, respectively. For the sake of notational simplicity, we have omitted explicit reference to retardation effects. These have been approximately included in the way described in Ref. 6.

Using the energy-momentum relation

$$[\epsilon+m-U_o^{\mathrm{HF}}(k_F,k)]^2=k^2\left[1+\frac{U_v^{\mathrm{HF}}(k_F,k)}{k}\right]^2+[m+U_s^{\mathrm{HF}}(k_F,k)]^2\ , \tag{2.4}$$

the momentum dependence of each component of the Hartree-Fock potential $U^{\mathrm{HF}}$ can be transformed into a dependence upon the center-of-mass energy $\epsilon$

$$U_i^{\mathrm{HF}}=U_i^{\mathrm{HF}}(k_F;\epsilon)\quad (i=s,o,v)\ . \tag{2.5}$$

In order to construct the average nucleon-nucleus potential for a finite system, we introduce a local density approximation (LDA). In its simplest form, this approximation assumes that the components of the relativistic potential $U^{\mathrm{HF}}$ at the distance $r$ of the nuclear center takes the same value as in a uniform medium with a density equal to the local nuclear density. This yields

$$U_i^{\mathrm{HF}}(r;\epsilon)=U_i^{\mathrm{HF}}(k_F(r);\epsilon)\quad (i=s,o,v)\ , \tag{2.6}$$

where $k_F(r)$ is related to the empirical nuclear density distribution by

$$\rho(r)=\frac{2}{3\pi^2}k_F^{\,3}(r)\ . \tag{2.7}$$

The quantity $U_v^{\mathrm{HF}}$ is smaller than $U_s^{\mathrm{HF}}$ and $U_o^{\mathrm{HF}}$ by one order of magnitude.[6] Moreover, it practically does not influence the elastic scattering phase shifts in a finite system[6]; accordingly we shall henceforth disregard it. Then the Dirac-Hartree-Fock equation satisfied by the scattering wave function in the framework of the LDA reads

$$\{\vec{\alpha}\cdot\vec{p}+\gamma^0[m+U_s^{\mathrm{HF}}(r;\epsilon)+\gamma^0 U_o^{\mathrm{HF}}(r;\epsilon)]\}\phi(\vec{r};\epsilon)=(\epsilon+m)\phi(\vec{r};\epsilon)\ . \tag{2.8}$$

A local density approximation developed in the framework of the Hartree approximation leads to an equation similar to Eq. (2.6) but without energy dependence

$$U_i^H(r)=U_i^H[k_F(r)]\quad (i=s,o)\ . \tag{2.9}$$

### B. Weakness of the LDA

In this section, we exhibit what distinguishes the exact Hartree potentials for finite nuclei from those calculated via a local density approximation defined by Eqs. (2.7) and (2.9).

For a finite nucleus, the exact components of $U^H$ are written[3]

$$U_i^{\mathrm{FN}}(r)=\frac{g_i^{\,2}}{4\pi}\int\rho_i(r')v_i(|\vec{r}-\vec{r}'|)d\vec{r}'\quad (i=s,o)\ , \tag{2.10}$$

where the upper index FN refers to finite nucleus. The quantities

$$v_s(r)=-r^{-1}(e^{-m_\sigma r}-e^{-\Lambda_\sigma r}) , \tag{2.11a}$$

$$v_o(r)=r^{-1}(e^{-m_\omega r}-e^{-\Lambda_\omega r}) , \tag{2.11b}$$

denote the nucleon-nucleon interaction due to the exchange of the meson $\sigma$ and of the meson $\omega$, respectively; $m_i$ $(i=\sigma,\omega)$ is the mass of the exchanged meson and $\Lambda_i$ refers to a cutoff momentum. The nucleon distribution density and the scalar density are denoted by $\rho_o(r)=\rho(r)$ and by $\rho_s(r)$, respectively. Finally, $g_s^2$ $(g_o^2)$ represents the $\sigma$ $(\omega)$ meson coupling constant.

In nuclear matter of constant density $\rho$, the potentials (2.10) become $r$ independent. We denote them by $U_i^{\rm NM}$. One has

$$U_i^{\rm NM}=\frac{g_i^2}{4\pi}\rho_i\int v_i(r')d\vec{r}' \quad (i=s,o) . \tag{2.12}$$

From these potentials, the LDA prescription (2.7) and (2.9) gives the following approximation for the potentials for a finite system:

$$U_i^{\rm LDA}(r)=\frac{g_i^2}{4\pi}\rho_i(r)\int v_i(r')d\vec{r}' . \tag{2.13}$$

Equations (2.10) and (2.13) show that the potentials $U_i^{\rm LDA}(r)$ would be identical to the exact potentials $U_i^{\rm FN}(r)$ if and only if the interactions $v_i(r)$ had a zero range. This condition is not fulfilled in practice. Therefore we can expect that the usual LDA defined in Sec. II A will give a rather good approximation of the Hartree approximation in the inner region of the nucleus, while it will lead to poorer results at the nuclear surface.

## III. IMPROVED LOCAL DENSITY APPROXIMATION

A possible way for improving the LDA defined in Sec. II consists of including the effect of a range in the expression of the relativistic potentials.[10] This amounts to folding the various components $U_i^{\rm LDA}(r)$ of the average nucleon-nucleus potential calculated in the LDA by the corresponding nucleon-nucleon interaction $v_i(r)$

$$U_i^{\rm ILDA}(r)=C_i\int d\vec{r}'U_i^{\rm LDA}(r')v_i(|\vec{r}-\vec{r}'|) , \tag{3.1}$$

where the upper index "ILDA" refers to "improved LDA." The constants $C_i$ are chosen in such a way that $U_i^{\rm ILDA}=U^{\rm LDA}$ in a uniform medium, namely

$$C_i=\left[\int d\vec{r}'v_i(r')\right]^{-1} . \tag{3.2}$$

In the Hartree approximation, Eqs. (3.1) and (2.10) are strictly equivalent. Indeed, we find, using Eq. (2.13),

$$\begin{aligned}U_i^{\rm ILDA}(r)&=\left[\int d\vec{r}'v_i(r')\right]^{-1}\int d\vec{r}''\frac{g_i^2}{4\pi}\rho_i(r'')\left[\int d\vec{r}'''v_i(r''')\right]v_i(|\vec{r}-\vec{r}''|)\\&=\frac{g_i^2}{4\pi}\int d\vec{r}''\rho_i(r'')v_i(|\vec{r}-\vec{r}''|)\\&\equiv U_i^{\rm FN}(r) .\end{aligned} \tag{3.3}$$

We apply Eq. (3.1) to the case of the Hartree-Fock potentials. We recall that, in the Hartree-Fock approximation, the mesons $\sigma$ and $\omega$ both contribute to $U_s^{\rm HF}(r;\epsilon)$ and $U_o^{\rm HF}(r;\epsilon)$.[6] Therefore, using the nucleon-nucleon interaction given by Eqs. (2.11), we write

$$U_i^{j\rm ILDA}(r;\epsilon)=C^j\int d\vec{r}'U_i^{j\rm LDA}(r';\epsilon)\,|\vec{r}-\vec{r}'|^{-1}[\exp(-m_j|\vec{r}-\vec{r}'|)-\exp(-\Lambda_j|\vec{r}-\vec{r}'|)]$$
$$(i=s,o;\ j=\sigma,\omega) , \tag{3.4}$$

with

$$\begin{aligned}C^j&=\left[\int d\vec{r}r^{-1}(e^{-m_jr}-e^{-\Lambda_jr})\right]^{-1}\\&=\frac{1}{4\pi}\Lambda_j^2m_j^2/(\Lambda_j^2-m_j^2) \quad (j=\sigma,\omega) .\end{aligned} \tag{3.5}$$

In Eq. (3.4), $U_i^{j\rm LDA}(r;\epsilon)$ represents the contribution of the meson $j$ to the approximate Hartree-Fock potential $U_i^{\rm HF}(r;\epsilon)$ defined by Eq. (2.6). The new Hartree-Fock potentials for finite nuclei are then written

$$\begin{aligned}U_s^{\rm HF}(r;\epsilon)&\equiv U_s^{\rm ILDA}(r;\epsilon)\\&=U_s^{\sigma\rm ILDA}(r;\epsilon)+U_s^{\omega\rm ILDA}(r;\epsilon) ,\end{aligned} \tag{3.6}$$

TABLE I. Coupling strengths and masses of the mesons $\sigma$ and $\omega$ used in our Hartree-Fock calculations (cutoff energy $\Lambda_\sigma=\Lambda_\omega=1530$ MeV).

| $g_s^2/4\pi$ | $g_o^2/4\pi$ | $m_\sigma$ (MeV) | $m_\omega$ (MeV) |
|---|---|---|---|
| 7.47 | 10.15 | 550 | 782.8 |

$$U_o^{\mathrm{HF}}(r;\epsilon)\equiv U_o^{\mathrm{ILDA}}(r;\epsilon) = U_o^{\sigma\mathrm{ILDA}}(r;\epsilon)+U_o^{\omega\mathrm{ILDA}}(r;\epsilon)\ . \tag{3.7}$$

## IV. NUMERICAL RESULTS

### A. Input parameters

In order to calculate the Hartree-Fock potentials defined by Eq. (2.6) or by Eqs. (3.4)–(3.7), we use parameters that we have adjusted to reproduce the empirical saturation point of nuclear matter, namely, $\rho_o=0.17$ nucleon/fm$^3$, average binding energy per nucleon $B/A=-15.6$ MeV.[8] As $U_i^{\mathrm{ILDA}}=U_i^{\mathrm{LDA}}$ in a uniform system, these parameters are strictly identical for the LDA or for the improved LDA. They are listed in Table I.

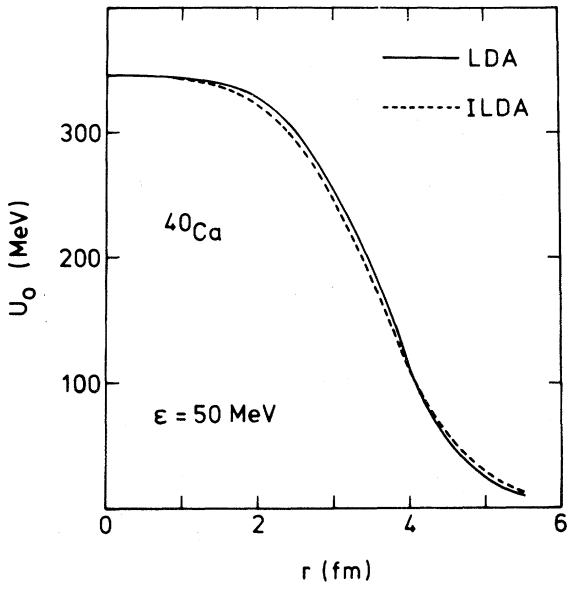


FIG. 1. Radial shape of the Hartree-Fock component $U_o^{\mathrm{HF}}(r;\epsilon)$ for $\epsilon=50$ MeV, in the case of $^{40}$Ca. The full curve corresponds to the LDA while the dotted curve shows values of the potential in the improved LDA.

We show results for the elastic scattering of a nucleon by the nucleus $^{40}$Ca. We take the empirical density distribution $\rho(r)$ from Ref. 11.

In Fig. 1, we exhibit the radial shape of the relativistic Hartree-Fock component $U_o^{\mathrm{HF}}(r;\epsilon)$ at $\epsilon=50$ MeV in the LDA (full curve) and in the improved LDA (dotted curve). The latter approximation mostly modifies the diffuseness of the potential. A similar result is obtained for the scalar component $U_s^{\mathrm{HF}}$.

### B. Energy dependence of the strengths of the scalar and vector components of the Dirac potential

Recently, Arnold and collaborators have exhibited that the rendering of the experimental data of elastic nucleon-nucleus scattering mainly determines the energy dependent ratio $R(\epsilon)$ between the strength of the vector and of the scalar components of the single-particle potential

$$R(\epsilon)=-\frac{\int U_o(r;\epsilon)d\vec{r}}{\int U_s(r;\epsilon)d\vec{r}}\ . \tag{4.1}$$

Moreover, it has appeared from the $p$-$^{40}$Ca (Ref. 12) and the $p$-$^4$He (Ref. 13) elastic scattering data analyses that this ratio $R$ decreases linearly with increasing laboratory energy $T_p$. For a comparison with the theoretical prediction, one should express the ratio $R$ as a function of the center-of-mass energy $\epsilon$. The two quantities $T_p$ and $\epsilon$ are related by the following equation[14,15]:

$$(\epsilon^2+2m\epsilon)^{1/2}=\frac{Am}{\epsilon+(A+1)m}(T_p^{\,2}+2mT_p)^{1/2}\ , \tag{4.2}$$

where $A$ denotes the number of nucleons in the target. From this equation, we can see that the linear dependence upon energy remains valid in the center-of-mass system for a medium-weight nucleus as $^{40}$Ca or for a heavy nucleus. However, for a light nucleus such as $^4$He, the ratio $R$ decreases more rapidly with increasing energy $\epsilon$ than with increasing energy $T_p$.

The energy dependence of $R$ implies that the two components $U_s$ and $U_o$ of the single-particle potential depend also upon energy. This entails the introduction of at least the Fock terms when these two potentials are calculated in a microscopic approach. In Fig. 2, we have represented by the full curve the ratio $R$ calculated in the Hartree-Fock approximation via the LDA defined by Eqs. (2.6) and (2.7). It

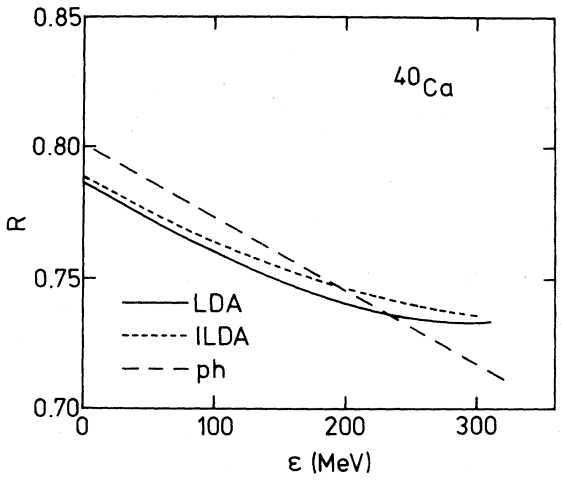


FIG. 2. Ratio $R$ of the strengths of the vector and scalar components versus energy in the case of $^{40}$Ca. The full line corresponds to a LDA prescription while the dotted curve shows results for the improved LDA. The dashed curve comes from Ref. 12.

is in semiquantitative agreement with the empirical finding of Ref. 12 (dashed curve). The agreement is improved when the Hartree-Fock potentials are calculated in the improved LDA defined by Eqs. (3.4)–(3.7). This is exhibited by the dotted curve in Fig. 2. In both the LDA and the improved LDA, the ratio $R$ goes to a constant when $\epsilon \to \infty$. This is explained by the fact that the Fock contributions tend towards zero when $\epsilon$ becomes larger than $\simeq$300 MeV (Ref. 6). Consequently, for large $\epsilon$ the quantities $U_s$ and $U_o$ take their Hartree value and $R$ becomes independent upon energy. This discrepancy with experimental evidence is not yet explained. The introduction of heavier mesons might be useful.

### C. Schrödinger-equivalent potential

Since experimental data are usually analyzed in the framework of a nonrelativistic optical model, it is useful to construct a "Schrödinger-equivalent potential" which can be associated to the real part of the optical-model potential. In the context of a LDA, this average potential is obtained by eliminating the small components of the scattering wave function in the Dirac equation (2.8). After some manipulation[9,3] one finds that the modified wave function

$$\tilde{\phi}_> = [\epsilon + 2m + U_s(r;\epsilon) - U_o(r;\epsilon)]^{-1/2} \phi_> , \tag{4.3}$$

where $\phi_>$ represents the large components of $\phi$, satisfies the following Schrödinger-type equation

$$\left[ \frac{\vec{p}^{\,2}}{2m} + \hat{U}_e(r;\epsilon) \right] \tilde{\phi}_> = \frac{k_\infty^{\,2}}{2m} \tilde{\phi}_> \tag{4.4}$$

with the relativistic asymptotic momentum $k_\infty$ defined by

$$k_\infty^{\,2} = 2m\epsilon + \epsilon^2 . \tag{4.5}$$

We have called[9] the quantity $\hat{U}_e(r;\epsilon)$ the Schrödinger-equivalent potential since it yields the same elastic scattering phase shifts as the original Dirac potential. It is the sum of a central part

$$U_e(r;\epsilon) \simeq [U_s(r;\epsilon) + U_o(r;\epsilon)] \times \left[ 1 + \frac{U_s(r;\epsilon) - U_o(r;\epsilon)}{2m} \right] + U_o(r;\epsilon) \frac{\epsilon}{m} \tag{4.6}$$

and of a spin-orbit component

$$\frac{1}{r} U_{so}(r;\epsilon) \vec{\sigma} \cdot \vec{L} = - \frac{1}{2mrD(r;\epsilon)} \frac{d}{dr} D(r;\epsilon) \tag{4.7}$$

with

$$D(r;\epsilon) = 2m + \epsilon + U_s(r;\epsilon) - U_o(r;\epsilon) . \tag{4.8}$$

The quantities defined by Eqs. (4.6)–(4.8) can be identified with the central and spin-orbit components of the optical-model potential, respectively. In Eqs. (4.3)–(4.8) we have dropped the upper in-

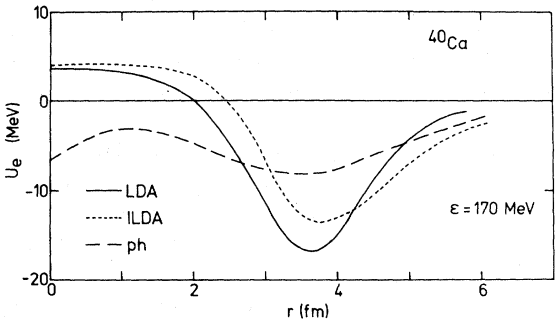


FIG. 3. Radial shape of the central part of the optical-model potential for $\epsilon = 170$ MeV in the case of $^{40}$Ca. The full line shows the Schrödinger-equivalent potential defined by Eq. (4.6), calculated in the LDA, while the dotted curve corresponds to the improved LDA. The dashed curve results from the empirical analyses of Refs. 12 and 16.

dex HF; we have also neglected the derivative terms in Eq. (4.6), which are very small. Recent scattering data analyses[12,14,16–18] have shown that the central part of the optical potential exhibits the striking feature of being repulsive inside the nucleus while it remains attractive at the nuclear surface at intermediate energy. This "wine-bottle bottom shape" had been predicted in the framework of the Hartree approximation.[3,9] In Fig. 3, we compare the shape of the central part of the empirical optical potential emerging from the $p$-$^{40}$Ca elastic scattering data analyses at $T_p = 180$ MeV (dashed curve)[12,16] with Schrödinger-equivalent potentials defined by Eq. (4.6). The full line corresponds to Hartree-Fock potentials $U_s(r;\epsilon)$ and $U_o(r;\epsilon)$ calculated via the LDA [Eq. (2.6)] while the dotted curve refers to the improved LDA [Eqs. (3.4)–(3.7)]. Both potentials have been calculated for $\epsilon = 170$ MeV which corresponds to a laboratory energy of 180 MeV, as can be found from Eq. (4.2). We note that the improved LDA yields a better agreement with experiment, mainly at the nuclear surface where the well is more shallow.

The full curve in Fig. 4 of Ref. 8 represents the volume integral per nucleon of the Schrödinger-equivalent potential [Eq. (4.6)] of $^{40}$Ca with Hartree-Fock potentials calculated in the local density approximation with effective parameters of Table I. This approximation is in fair agreement with the empirical values at low and at intermediate energy. Since the improved LDA only modifies the tail of the Hartree-Fock potentials (see Fig. 1), the volume integral of $U_e$ calculated in this approximation takes roughly the same values than in the LDA.

On the other hand, Fig. 4 shows that the mean square radius $\langle r^2(\,|\,U_e\,|\,)\rangle$ takes values too small in the LDA (full curve) while the agreement between theory and experiment is significantly improved when $\langle r^2(\,|\,U_e\,|\,)\rangle$ is calculated in the improved LDA (dotted curve).

The LDA and the improved LDA mainly take their difference in the description of the nuclear surface. Since the spin-orbit component is a surface potential, it is interesting to compare the values obtained for this quantity in the two approximations. In Fig. 5, we have represented by the full curve the spin-orbit potential $U_{so}(r;\epsilon)$ defined by Eqs. (4.7) and (4.8) and calculated in the LDA. The dotted curve corresponds to the improved LDA. The long dashes show the average of the empirical spin-orbit potentials found by van Oers.[20] We note that the two theoretical curves are in very good agreement with the empirical one.

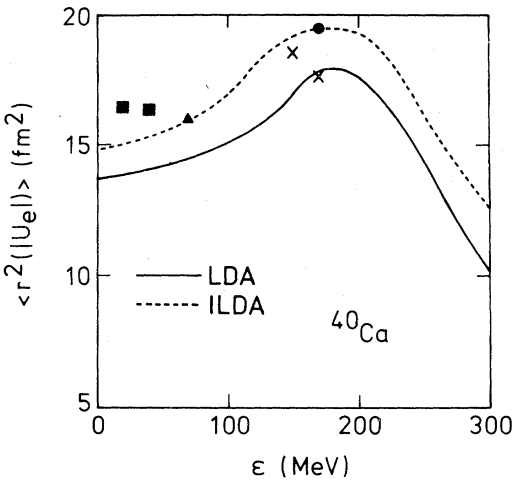


FIG. 4. Energy dependence of the mean square radius $\langle r^2(\,|\,U_e\,|\,)\rangle$ in the LDA (full line) and in the improved LDA (dotted curve), in the case of $^{40}$Ca. The empirical points come from Refs. 10 (squares), 19 (triangle), and 15 (crosses and circle).

## V. SUMMARY

We have introduced an improved local density approximation in order to evaluate the Hartree-Fock single-nucleon potentials for finite nuclei from those calculated in symmetric nuclear matter. This approximation is "improved" in the sense that it is a better approximation at the nuclear surface than the LDA defined in Sec. II. Both the LDA and the improved LDA reproduce well the shape and the depth of the spin-orbit component of the optical potential. In most cases, however, the improved LDA

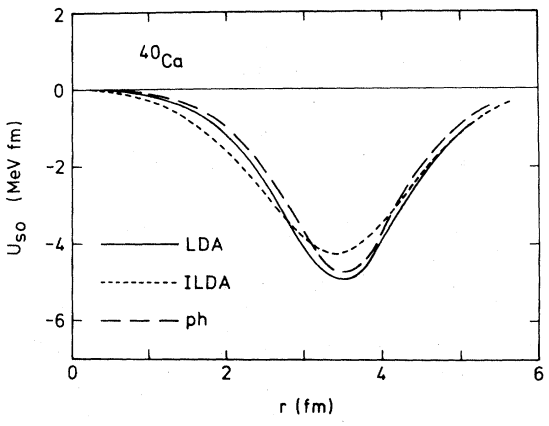


FIG. 5. Spin-orbit potential $U_{so}(r;\epsilon)$ [Eqs. (4.7) and (4.8)] for $^{40}$Ca at $\epsilon = 50$ MeV, in the LDA (full curve) and in the improved LDA (dotted curve). The long dashes show the average of the empirical spin-orbit potentials found by van Oers (Ref. 20).

yields better agreement with empirical results than the usual LDA. In particular, we have shown that the improved LDA makes more shallow the surface pocket of the central part of the optical potential at intermediate energy and increases the values of the mean square radius $\langle r^2( \mid U_e \mid ) \rangle$. It also improves the agreement between the calculated and empirical values of the ratio $R(\epsilon)$ defined by Eq. (4.1).

We gratefully acknowledge stimulating discussions with C. Mahaux.

[1]L. D. Miller and A. E. S. Green, Phys. Rev. C 5, 241 (1972).
[2]J. D. Walecka, Ann. Phys. (N. Y.) 83, 491 (1974).
[3]M. Jaminon, C. Mahaux, and P. Rochus, Phys. Rev. C 22, 2027 (1980).
[4]L. D. Miller, Phys. Rev. C 12, 710 (1975).
[5]R. Brockmann, private communication.
[6]M. Jaminon, C. Mahaux, and P. Rochus, Nucl. Phys. A365, 371 (1981).
[7]L. G. Arnold and B. C. Clark, Phys. Lett. 84B, 46 (1979).
[8]M. Jaminon and C. Mahaux, Phys. Rev. C 24, 1353 (1981).
[9]M. Jaminon, C. Mahaux, and P. Rochus, Phys. Rev. Lett. 43, 1097 (1979).
[10]J.-P. Jeukenne, A. Lejeune, and C. Mahaux, Phys. Rev. C 16, 80 (1977).
[11]J. W. Negele, Phys. Rev. C 1, 1260 (1970).
[12]L. G. Arnold, B. C. Clark, E. D. Cooper, M. S. Sherif, D. A. Hutcheon, P. Kitching, J. M. Cameron, R. P. Liljestrand, R. N. McDonald, W. J. McDonald, C. A. Miller, G. C. Neilson, W. C. Olsen, D. M. Sheppard, G. M. Stinson, D. K. McDaniels, J. R. Tinsley, R. L. Mercer, L. W. Swenson, P. Schwandt, and C. E. Stronach, Phys. Rev. C (to be published).
[13]L. G. Arnold, B. C. Clark, and R. L. Mercer, Phys. Rev. C 19, 917 (1979).
[14]H. O. Meyer, P. Schwandt, G. L. Moake, and P. P. Singh, Phys. Rev. C 23, 616 (1981).
[15]A. Nadasen, P. Schwandt, P. P. Singh, W. W. Jacobs, A. D. Bacher, P. T. Debevec, M. D. Kaitchuck, and J. T. Meek, Phys. Rev. C 23, 1023 (1981).
[16]L. G. Arnold, B. C. Clark, R. L. Mercer, and P. Schwandt, Phys. Rev. C 23, 1949 (1981).
[17]H. O. Meyer, J. Hall, W. W. Jacobs, P. Schwandt, and P. P. Singh, Phys. Rev. C 24, 1782 (1981).
[18]D. A. Hutcheon, J. M. Cameron, R. P. Liljestrand, P. Kitching, C. A. Miller, W. J. McDonald, D. M. Sheppard, W. C. Olsen, G. C. Neilson, H. S. Sherif, D. K. McDaniels, J. R. Tinsley, L. W. Swenson, P. Schwandt, C. E. Stronach, and L. Ray, Phys. Rev. Lett. 47, 315 (1981).
[19]W. T. H. van Oers and H. Haw, Phys. Lett. 45B, 227 (1973).
[20]W. T. H. van Oers, Phys. Rev. C 3, 1550 (1971).